Biol. Cybern. 87, 102–115 (2002)
DOI 10.1007/s00422-002-0322-5

Biological Cybernetics

Desynchronization of brain rhythms with soft phase-resetting techniques

Peter A. Tass

Institute of Medicine, Research Centre Jülich, 52425 Jülich, Germany

Received: 3 July 2001 / Accepted in revised form: 7 February 2002

Abstract. Composite stimulation techniques are presented here which are based on a soft (i.e., slow and mild) reset. They effectively desynchronize a cluster of globally coupled phase oscillators in the presence of noise. A composite stimulus contains two qualitatively different stimuli. The first stimulus is either a periodic pulse train or a smooth, sinusoidal periodic stimulus with an entraining frequency close to the cluster's natural frequency. In the course of several periods of the entrainment, the cluster's dynamics is reset (restarted), independently of its initial dynamic state. The second stimulus, a single pulse, is administered with a fixed delay after the first stimulus in order to desynchronize the cluster by hitting it in a vulnerable state. The incoherent state is unstable, and thus the desynchronized cluster starts to resynchronize. Nevertheless, resynchronization can effectively be blocked by repeatedly delivering the same composite stimulus. Previously designed stimulation techniques essentially rely on a hard (i.e., abrupt) reset. With the composite stimulation techniques based on a soft reset, an effective desynchronization can be achieved even if strong, quickly resetting stimuli are not available or not tolerated. Accordingly, the soft methods are very promising for applications in biology and medicine requiring mild stimulation. In particular, it can be applied to effectively maintain incoherency in a population of oscillatory neurons which try to synchronize their firing. Accordingly, it is explained how to use the soft techniques for (i) an improved, milder, and demand-controlled deep brain stimulation for patients with Parkinson's disease or essential tremor, and for (ii) selectively blocking gamma activity in order to manipulate visual binding.

1 Introduction

Synchronization processes abound in neuroscience (Eckhorn et al. 1988; Gray and Singer 1989) and medicine (Llinás and Jahnsen 1982; Bergman et al. 1994; Volkmann et al. 1996). Stimulation is a major experimental tool for studying and manipulating synchronization under physiological as well as pathological conditions. Let us consider two examples in the following.

Deep brain stimulation. Parkinsonian resting tremor appears to be caused by a cluster of neurons located in the thalamus and the basal ganglia which fire synchronously at a frequency similar to that of the tremor (Llinás and Jahnsen 1982; Pare et al. 1990; Lenz et al. 1994). By contrast, under physiological conditions the neurons in this cluster fire incoherently (Nini et al. 1995). In patients with Parkinson's disease (PD) this cluster acts like a pacemaker and activates premotor areas (premotor cortex and supplementary motor area) and the motor cortex (Alberts et al. 1969; Lamarre et al. 1971; Bergman et al. 1994; Nini et al. 1995; Volkmann et al. 1996), where the latter synchronize their oscillatory activity (Tass et al. 1998). Similarly, essential tremor also appears to be caused by a central cluster of synchronously firing neurons, although they are located in different brain areas compared to PD (Elble and Koller 1990).

In patients with advanced PD or with essential tremor who do not respond to drug therapy any more, electrodes are chronically implanted within a particular neuronal cluster of the brain with millimeter precision (Benabid et al. 1991; Blond et al. 1992). Up to now, a permanent high-frequency stimulation with a high-frequency (>100 Hz) periodic pulse train has been administered via the deep brain electrodes in order to suppress the pathological synchronized activity of the pacemaker-like cluster which, in turn, suppresses the peripheral tremor (Benabid et al. 1991; Blond et al. 1992). The method presented here can be used to develop a mild and efficient, demand-controlled deep brain stimulation technique for patients with PD or essential tremor.

Sensory manipulation of visual binding. An important and still unsolved issue in neuroscience is the visual

Correspondence to: P. A. Tass
(e-mail: P.Tass@fz-juelich.de)

binding problem, which is the question of how information that is spatially distributed in the brain gets bound together to form a meaningful pattern of perception. It was suggested that the mechanism which realizes the visual binding is the synchronization of the firing in the gamma frequency range (30–80 Hz, especially around 40 Hz) of neurons coding for specific features belonging to an object in the visual field (Eckhorn et al. 1988; Gray and Singer 1989). In anesthetized cat (Eckhorn et al. 1988; Gray and Singer 1989) and awake monkey (Kreiter and Singer 1992; Eckhorn et al. 1993) it was observed that smoothly moving stimuli induce sustained gamma oscillations in different visual cortical areas which are synchronized in phase. While rapidly changing stimuli evoke stimulus-locked fast and transient responses, the gamma oscillations occur with longer and more variable latencies (Gray et al. 1992).

The functional role of gamma oscillations in visual binding is still a matter of debate (cf. Ghose and Maunsell 1999; Riesenhuber and Poggio 1999). For instance, due to the latencies of these oscillations their contribution to visual binding in rapidly changing scenes is questionable (Ghose and Freeman 1992). To address this issue, in visual cortical areas of anesthetized cat sustained gamma oscillations were produced by a slowly drifting visual grating pattern and then perturbed by intermingled sudden random accelerations of the grating (Kruse and Eckhorn 1996). With increasing amplitude of the random perturbations the corresponding evoked fast responses increased, whereas the amplitude of gamma oscillations gradually decreased. Kruse and Eckhorn (1996) suggest that this suppression of gamma oscillations is necessary for switching between different percepts.

To manipulate gamma oscillations without additional, perturbing stimuli, entraining and resonance effects of visual stimuli were studied. It was shown that visual stimuli flickering at a frequency that is close to the resonance frequency of 40 Hz strongly entrain neuronal populations in cat (Rager and Singer 1998) and human (Herrmann 2001) visual cortex. Moreover, Kanisza-like visual stimuli flickering at the resonance frequency (40 Hz) are more rapidly processed by the brain than stimuli flickering at other frequencies (Elliot and Müller 1998), and they are connected with reduced latencies of stimulus-evoked gamma responses as measured with electroencephalography (Elliot et al. 2000). The novel soft phase-resetting technique shown here may be used for visual stimulation to block gamma activity in order to selectively study its role in visual binding processes. For this, the same visual stimulus has to be administered with an appropriate timing and intensity sequence. In this way it may be possible to study how the stability of a single percept is manipulated by desynchronizing gamma oscillations without using additional stimuli related to different percepts. In other words, the relationship between a single percept and gamma oscillations can be studied without switching between different percepts.

The present study is based on a stochastic phase-resetting approach (Tass 1999). To investigate desynchronizing effects of pulsatile stimuli, the concept of phase resetting (Winfree 1980) was extended to populations of noninteracting (Tass 1996a, b) and interacting (Tass 1999, 2000) oscillators in the presence of random forces. With this aim in view, limit-cycle oscillators are approximated by phase oscillators (Kuramoto 1984), and desynchronization is caused by stimuli that exclusively affect the oscillators' phases. A fully synchronized cluster of oscillators is desynchronized by a single pulse of the correct intensity and duration provided the pulse hits the cluster in a vulnerable phase range that corresponds to only a small fraction (5% or even less) of a period of the oscillation. Of course, this is tricky to realize under noisy experimental conditions typically encountered in biological systems. Moreover, different stimulation parameters have to be used to desynchronize a cluster which is not in its fully synchronized state (Tass 1999, 2001a).

By contrast, stimulation techniques were recently presented which effectively desynchronize a cluster of oscillators irrespective of the cluster's dynamic state at the beginning of the stimulation (Tass 2001a–c). These methods are much more appropriate for medical or biological applications and have one common feature: the stimulus contains two qualitatively different stimuli. The first stimulus is either a strong single pulse (Tass 2001a, c) or a high-frequency pulse train (with a frequency that exceeds the cluster's natural frequency by a factor of 20 or more; Tass 2001b). The strong first stimulus causes a *hard reset* (i.e., abrupt reset) during which the collective oscillation runs for less than one period. After this reset the cluster restarts in a stereotypical way. The second, weaker stimulus is a single pulse that is administered after a constant time delay and desynchronizes by hitting the cluster in a vulnerable state.

It has to be stressed that a hard reset requires that the stimulus strongly affects the stimulated system without causing any damage. In biology and medicine, however, there are many systems for which direct and strong stimuli are not available or that do not tolerate strong stimuli (Stoney et al. 1968; Winfree 1980). To overcome this problem, a novel, effectively desynchronizing *composite stimulus* is presented here. It consists of two qualitatively different stimuli. The first stimulus causes a soft reset, and is either a periodic pulse train or a smooth periodic (e.g., sinusoidal) stimulus, where in both cases the entraining frequency is close to the natural frequency of the cluster (before stimulation). During this *soft reset* (i.e., slow reset), the collective oscillation is not quickly abrupted. By contrast, in the course of this entrainment the influence of the initial dynamic state at the beginning of the stimulation fades away while the collective oscillation runs through several periods. The second stimulus is a single pulse which follows after a constant time delay and hits the cluster in a vulnerable state, in this way desynchronizing it.

Since such a combined stimulus desynchronizes a cluster no matter at which initial dynamic state it is administered, this method can be used to block the cluster's resynchronization. To this end a combined stimulus has to be administered repeatedly, whenever

the cluster becomes synchronized again. This novel technique may find several significant applications in biology and medicine. In this article I shall focus on demand-controlled deep brain stimulation and on sensory manipulation of visual binding with desynchronizing visual stimulation. A part of the analysis of the dynamics caused by a composite stimulus with pulsatile entrainment was presented in a rapid communication (Tass 2002).

2 Stochastic approach

2.1 Model

The dynamics of a neuronal population can be modeled by means of networks of phase oscillators. A detailed explanation of this approach is presented in Kuramoto (1984), Ermentrout and Kopell (1991), Grannan et al. (1993), and Hansel et al. (1993). The dynamics of a cluster of coupled phase oscillators subjected to a stimulus S and to random forces is governed by the *Langevin equation*

$$\dot{\psi}_j = \Omega + \frac{1}{N}\sum_{k=1}^{N}\Gamma(\psi_j - \psi_k) + X(t)S(\psi_j) + F_j(t) \ , \qquad (1)$$

where ψ_j denotes the phase of the jth phase oscillator, i.e., the jth model neuron (Tass 1999). For the sake of simplicity all oscillators have the same eigenfrequency: $\omega_j = \Omega$. The global coupling is a 2π-periodic function. For the time being we consider a simple sine coupling of the form

$$\Gamma(\psi_j - \psi_k) = -K\sin(\psi_j - \psi_k) \ , \qquad (2)$$

where K is a nonnegative coupling constant. This type of coupling is sufficient in this study, because we focus on a cluster of oscillators synchronized in phase. The influence of cosine couplings such as $\cos(\psi_j - \psi_k)$ and $\cos 2[(\psi_j - \psi_k)]$ is discussed in Sect. 7. Sine coupling terms of second and higher order such as $\sin[2(\psi_j - \psi_k)]$ and $\sin[3(\psi_j - \psi_k)]$ give rise to noisy cluster states where the population consists of distinct phase-locked clusters. The stimulation techniques presented in this article also effectively desynchronize cluster states. Actually, the mechanism by which cluster states are desynchronized is practically the same as the desynchronizing mechanism for the in-phase synchronized cluster (see Sect. 7).

The impact of an electrical stimulus on a single neuron depends on the neuron's phase at which the stimulus is administered (Best 1979; Guttman et al. 1980). Accordingly, the stimulus is modelled by a 2π-periodic, time-independent function $S(\psi_j) = S(\psi_j + 2\pi)$. We first assume that the stimulus is of lowest order and defined by

$$S(\psi_j) = I\cos(\psi_j) \ , \qquad (3)$$

where I is a constant intensity parameter. The effect of higher-order terms of S is discussed in Sect. 7. Switching the stimulator on and off is taken into account by

$$X(t) = \begin{cases} 1 & : \text{ stimulus is on at time } t \\ 0 & : \text{ stimulus is off at time } t \end{cases} . \qquad (4)$$

The random forces $F_j(t)$ are modelled by Gaussian white noise: $\langle F_j(t)\rangle = 0$ and $\langle F_j(t)F_k(t')\rangle = D\delta_{jk}\delta(t-t')$, with constant noise amplitude D.

To investigate the dynamics of (1) we first derive the corresponding *Fokker–Planck equation* which is an evolution equation for the *probability density* $f(\boldsymbol{\psi}, t)$, where $\boldsymbol{\psi}$ is the vector $(\psi_1, \ldots, \psi_N)$. $f(\boldsymbol{\psi}, t)\,\mathrm{d}\psi_1 \cdots \mathrm{d}\psi_N$ gives us the probability of finding the oscillators' phases in the intervals $\psi_k, \ldots, \psi_k + \mathrm{d}\psi_k$. In order to simplify the analysis we consider the dynamics on a more macrospcopic level of description by introducing the *average number density* $n(\psi, t) = \langle \tilde{\boldsymbol{n}}(\boldsymbol{\psi}; \psi)\rangle_t = \int_0^{2\pi}\cdots\int_0^{2\pi} \mathrm{d}\psi_1 \cdots \mathrm{d}\psi_N \, \tilde{\boldsymbol{n}}(\boldsymbol{\psi}; \psi) f(\boldsymbol{\psi}, t)$, where the number density is defined by $\tilde{\boldsymbol{n}}(\boldsymbol{\psi}; \psi) = \frac{1}{N}\sum_{k=1}^{N}\delta(\psi - \psi_k)$ (Kuramoto 1984). The probability density $f(\boldsymbol{\psi}, t)$ provides us with information concerning the phase of each single oscillator. By contrast, $n(\psi, t)$ tells us how many oscillators of the whole population most probably have phase ψ at time t.

With a little calculation we finally obtain the evolution equation for the average number density

$$\frac{\partial n(\psi,t)}{\partial t} = -\frac{\partial}{\partial\psi}\left\{ n(\psi,t)\int_0^{2\pi}\mathrm{d}\psi'\Gamma(\psi-\psi')n(\psi',t)\right\} - \frac{\partial}{\partial\psi}n(\psi,t)X(t)S(\psi) - \Omega\frac{\partial}{\partial\psi}n(\psi,t) + \frac{D}{2}\frac{\partial^2 n(\psi,t)}{\partial\psi^2} \ , \qquad (5)$$

which holds for large N (Tass 1999). For a detailed analytical and numerical investigation of (5), please refer to Tass (1999).

2.2 Spontaneously emerging synchrony

The time-dependent extent of synchronization is quantified by means

$$Z(t) = R(t)\exp[i\varphi(t)] = \int_0^{2\pi} n(\psi,t)\exp(i\psi)\mathrm{d}\psi \ , \qquad (6)$$

where $R(t)$ and $\varphi(t)$ are the real amplitude and the real phase of Z, respectively (Kuramoto 1984). Due to the normalization condition $\int_0^{2\pi} n(\psi,t)\mathrm{d}\psi = 1$, the amplitude fulfills $0 \le R(t) \le 1$ for all times t. Perfect in-phase synchronization corresponds to $R = 1$, whereas an incoherent state, given by $n(\psi,t) = 1/(2\pi)$, corresponds to $R = 0$. $Z(t)$ corresponds to the center of mass of the circularly aligned density $n(\psi,t)\exp(i\psi)$ in the Gaussian plane (Fig. 1).

To study the stimulation-induced dynamics, first the cluster's behavior without stimulation (i.e., $X(t) = 0$ in 4) has to be clarified. Let us assume that the coupling is given by (2). (The influence of higher-order coupling terms is explained in Sect. 7.) Noisy in-phase synchro-

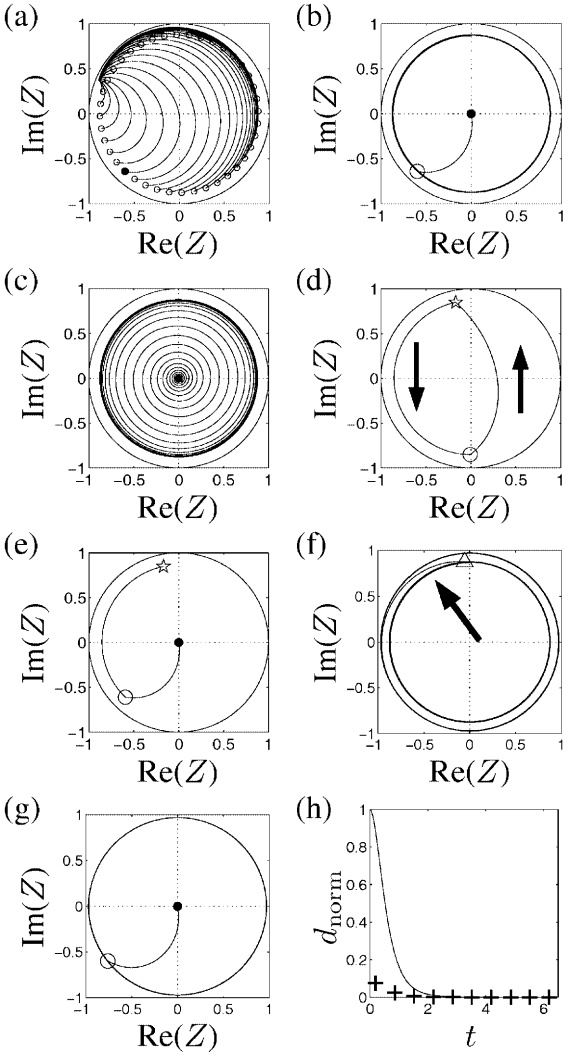

◀

Fig. 1a–h. Trajectories of Z from (6) are plotted in the Gaussian plane. In **a**–**e** the *unit circle* indicates the maximal range of $|Z|$. *Single pulse:* **a** Series of identical stimuli $S(\psi) = I\cos\psi$ (with $I = 7$) administered at different initial phases φ_{B} in the stable synchronized state (*open circles*). Z approaches the attractor Z^{stat} from (7) for $t \to \infty$. Only the stimulus administered at the vulnerable initial phase (*filled circles*) moves Z through the origin. Trajectory of Z before and during (**b**) and after (**c**) a desynchronizing single pulse (parameters as in **a**): **b** After running on its stable limit cycle (*inner circle*) in counterclockwise direction, Z is moved by the pulse into the origin ($Z = 0$). Stimulation starts at the *open circle* and ends at the *filled circle*. **c** After the stimulation the cluster spontaneously spirals back to its stable limit cycle. *Composite stimulus with pulsatile entrainment:* The periodic pulse train entrains the cluster so that Z performs a periodic motion (**d**): During each pulse of the train Z is shifted from $Z_{\mathrm{b}} = \lim_{k\to\infty} Z(t_{\mathrm{b},k})$ to $Z_{\mathrm{e}} = \lim_{k\to\infty} Z(t_{\mathrm{e},k})$ (*upward arrow*), while during each pause Z relaxes back from Z_{e} to Z_{b} (*downward arrow*). $t_{\mathrm{b},k}$ and $t_{\mathrm{e},k}$ denote the begin and end of the kth pulse. **e** At the end of the pulse train Z is sufficiently close to Z_{e} (*star*), and then relaxes back to its stable limit cycle. The desynchronizing pulse starts at the *open circle* and moves Z into the origin (*filled circle*). After the desynchronization Z spirals back to its stable limit cycle (as in **c**). *Composite stimulus with smooth entrainment:* **f** Before the stimulation Z is on its stable limit cycle (inner circle). The smooth stimulus starts at the *triangle* and rapidly moves Z to its entrained limit cycle (*outer circle*) where it oscillates with frequency ω_{s}. This transition is indicated by the *arrow*. **g** While Z is running on the entrained limit cycle, the second stimulus – a desynchronizing single pulse (with parameters as in **b**) – is administered at the *open circle* and moves Z into the origin (*filled circle*). **h** A periodic pulse train is applied to the fully synchronized cluster at $m = 100$ different initial phases equally spaced in $[0, 2\pi]$. $\mathrm{d}(t_{\mathrm{e},k})/\mathrm{d}(0)$ (*plus*), i.e., the normalized mean mutual distance of the order parameter Z at the end of the kth pulse during the pulse train, vanishes within a few periods where the pulse train starts at $t = 0$. Likewise the smooth periodic stimulus (8) is administered to the fully synchronized cluster at $m = 100$ different initial phases equally spaced in $[0, 2\pi]$. In this series of simulations $\mathrm{d}(t)/\mathrm{d}(0)$ (*solid line*) vanishes similarly. Model parameters were as follows. **a**–**h**: $\Gamma(x) = -\sin x$, $D = 0.4$, $\Omega = 2\pi$. Single pulse in **a**, **b**, **e**, and **g**: $S(\psi) = I\cos\psi$ with $I = 7$, pulse duration $T = 0.31$ in **b**, 0.33 in **e**, and 0.45 in **g**. Periodic pulse train (**d**): $S(\psi) = I\cos\psi$ with $I = 21$, pulse duration $T_1 = 0.2$, pause duration $T_2 = 0.47$, i.e., $\omega_{\mathrm{p}} = 3\pi$, number of pulses $M = 10$ (same results for $M > 100$). Smooth periodic pulse (**f**): $S(\psi) = I\cos(\psi - \omega_{\mathrm{s}} t)$ with $I = 7$, $\omega_{\mathrm{s}} = 3\pi$

nization emerges out of the ncoherent state $n = 1/(2\pi)$ due to a decrease of the noise amplitude D (Kuramoto 1984) or, analogously, because of an increase of the coupling strength (Tass 1999). When K exceeds its critical value $K^{\mathrm{crit}} = D$, Z from (6) becomes an *order parameter* (Haken 1983) which governs the dynamics of the other, infinitely many stable modes (i.e., frequency components) on the center manifold. In this way for $K > D$ a stable limit cycle $Z(t) = Y\exp[i(\Omega + \bar{\Omega})t]$ evolves, where Y is a complex constant, and $\bar{\Omega}$ is a real frequency shift term that depends on model parameters and vanishes if the coupling Γ contains no cosine terms, as in (2) (Tass 1999).

The cluster's collective dynamics will not only be visualized with the order parameter Z, but also by considering the collective firing. A single firing/bursting model neuron fires/bursts whenever its phase vanishes (modulo 2). Accordingly, the cluster's collective firing activity is given by the *firing density* $p(t) = n(0, t)$ which corresponds to quantities registered in neurophysiological experiments such as multiunit activity, local field potentials (LFP), and magnetic or electric fields measured with magnetoencephalography or electroencephalography.

3 Desynchronizing soft phase resetting

3.1 Desynchronizing single pulse

During a *single pulse*, $X(t) = 1$ and S is constant in time. If the stimulus S is sufficiently strong with respect to the coupling strength, $n(\psi, t)$ tends to a stationary density $n_{\mathrm{stat}}(\psi)$ for $t \to \infty$. The latter is the attractor of (5), irrespective of the initial state $n(\psi, 0)$ at which the stimulation starts (Tass 1999). Correspondingly, the order parameter is attracted by

$$Z^{\mathrm{stat}} = \int_0^{2\pi} n_{\mathrm{stat}}(\psi)\exp(i\psi)\mathrm{d}\psi \ , \qquad (7)$$

as shown in Fig. 1a, where the collective dynamics of the cluster is visualized by plotting the trajectory of Z in the Gaussian plane. Desynchronization corresponds to $Z = 0$. Hence, to desynchronize the synchronized cluster, the single pulse has to be administered at a critical

(vulnerable) initial phase and it has to be turned off as soon as Z reaches the origin of the Gaussian plane (Fig. 1b). The desynchronized state is unstable. Therefore after the desynchronizing stimulation, Z spirals back to its stable limit cycle, so that the cluster becomes synchronized again (Fig. 1c).

3.2 Pulsatile entrainment

A *composite stimulus with pulsatile entrainment* consists of two qualitatively different stimuli. The *first stimulus* is a train of M identical pulses. The kth pulse begins at $t_{b,k}$ and ends at $t_{e,k}$. The frequency of the pulse train is $\omega_p = 2\pi/(T_1 + T_2)$, where $T_1 = t_{e,k} - t_{b,k}$ and $T_2 = t_{b,k+1} - t_{e,k}$ are pulse duration and pause duration, respectively. The periodic pulse train resets the cluster by entrainment at a rate similar to the natural frequency of the cluster (before stimulation). Accordingly, the entraining frequency ω_p is of the same order of magnitude as Ω from (1). In the fully entrained state Z moves from $Z_b = \lim_{k\to\infty} Z(t_{b,k})$ to $Z_e = \lim_{k\to\infty} Z(t_{e,k})$ during each pulse, whereas Z relaxes back from Z_e to Z_b during each pause (Fig. 1d). The *second stimulus* follows after the pulse train with a constant time delay (corresponding to less than one period of the cluster's spontaneous oscillation), hits the cluster in a vulnerable state, and desynchronizes it by shifting Z into the origin (Fig. 1e).

3.3 Smooth Entrainment

A *composite stimulus with smooth entrainment* also contains two qualitatively different stimuli. The *first stimulus* is smooth, periodic, and explicitly timedependent. Instead of (3), we now start from a general ansatz for a first-order stimulus $S(\psi_j, t) = A(t)\sin(\psi_j) + B(t)\cos(\psi_j)$, where A and B are smooth periodic functions with period P: $A(t) = A(t+P)$ and $B(t) = B(t+P)$. Let us consider a special case connected with a straightforward dynamics that is sufficient to illustrate the main principle of smooth entrainment. To this end we assume that $A(t) = I\sin(\omega_s t)$ and $B(t) = I\cos(\omega_s t)$, which can be rewritten as

$$S(\psi_j, t) = I\cos(\psi_j - \omega_s t) \ , \tag{8}$$

where ω_s is the entraining frequency of the smooth entraining stimulus. Introducing a rotating coordinate system $\theta_j(t) = \psi_j(t) - \omega_s t$ for $j = 1, \ldots, N$, the Langevin equation (1) in this case reads $\dot{\theta}_j = \tilde{\Omega} + N^{-1}\sum_{l=1}^{N} \Gamma(\theta_j - \theta_l) + X(t)\tilde{S}(\theta_j) + F_j(t)$ with $\tilde{\Omega} = \Omega - \omega_s$ and $\tilde{S}(\theta_j) = I\cos\theta_j$. The Langevin equation in the rotating coordinate system is of the same form as (1). In particular, $\tilde{S}$ is no longer explicitly timedependent. Hence, the dynamics caused by the smooth periodic stimulus (8) in the rotating coordinate system $(\theta_1, \ldots, \theta_N)$ corresponds to the dynamics caused by the single pulse studied above with $S(\psi_j) = I\cos\psi_j$ in the initial coordinate system $(\psi_1, \ldots, \psi_N)$.

Accordingly, during the smooth periodic stimulation, Z tends to a fixed point in the rotating coordinate system provided I is sufficiently large. This fixed point is equivalent to a limit cycle of frequency ω_s in the initial coordinate system $(\psi_1, \ldots, \psi_N)$ (Fig. 1f). The second stimulus, a single pulse, is administered at a vulnerable state and causes a desynchronization by shifting Z into the origin of the Gaussian plane (Fig. 1g).

The very goal of both the pulsatile and the smooth entrainment is that the cluster's dynamics in the entrained state no longer depend on the initial dynamic conditions at the beginning of the entraining stimulation. To show this, a periodic pulse train (i.e., the first stimulus of the composite stimulus with pulsatile entrainment) is administered to the fully synchronized cluster at $m = 100$ different initial phases equally spaced in $[0, 2\pi]$. $Z^{(j)}(t)$ is the order parameter belonging to the simulation starting at the jth initial phase ($j = 1, \ldots, m$). The *mean mutual distance* of the order parameter in this series of simulations is given by

$$d(t) = \frac{2}{(m-1)m}\sum_{j=1}^{m}\sum_{k>j} |Z^{(j)}(t) - Z^{(k)}(t)| \ , \tag{9}$$

where $|x|$ denotes the absolute value of x, and the summation runs over all $(m-1)m/2$ pairs of different trajectories (Tass 2001b). Likewise, a smooth entraining stimulus (i.e., the first stimulus of the composite stimulus with smooth entrainment) is applied at $m = 100$ different, equally spaced initial phases, and $d(t)$ is determined. In the course of both the pulsatile and the smooth periodic entrainment d vanishes (Fig. 1h), which means that the entraining stimuli reset the cluster during several periods of the entrained oscillation. The reset guarantees that the influence of the initial dynamic conditions disappears. Therefore the desynchronizing effect of a composite stimulus is (practically) independent of the cluster's initial dynamic conditions, as demonstrated in Sect. 4.

4 Vulnerability to stimulation

4.1 Desynchronization

Let us compare the effect of a single pulse, a composite stimulus with pulsatile entrainment, and a composite stimulus with smooth entrainment on a cluster in the stable synchronized state, where $\phi_B = \varphi_B/(2\pi) \bmod 1$, which is the phase of Z at the beginning of the stimulation, is varied within one cycle (Fig. 2). The dynamics is visualized with the amplitude R of the order parameter from (6) and with the firing density $p(t) = n(0, t)$; i.e., the number density of all firing neurons, where the single neuron fires whenever its phase equals 0 mod 2π.

Obviously, the single pulse causes a desynchronization only provided it hits Z at or close to a vulnerable phase $\phi_B^{crit} \approx 0.38$ (Fig. 2a, b). By contrast, the composite stimuli temporarily desynchronize the cluster no

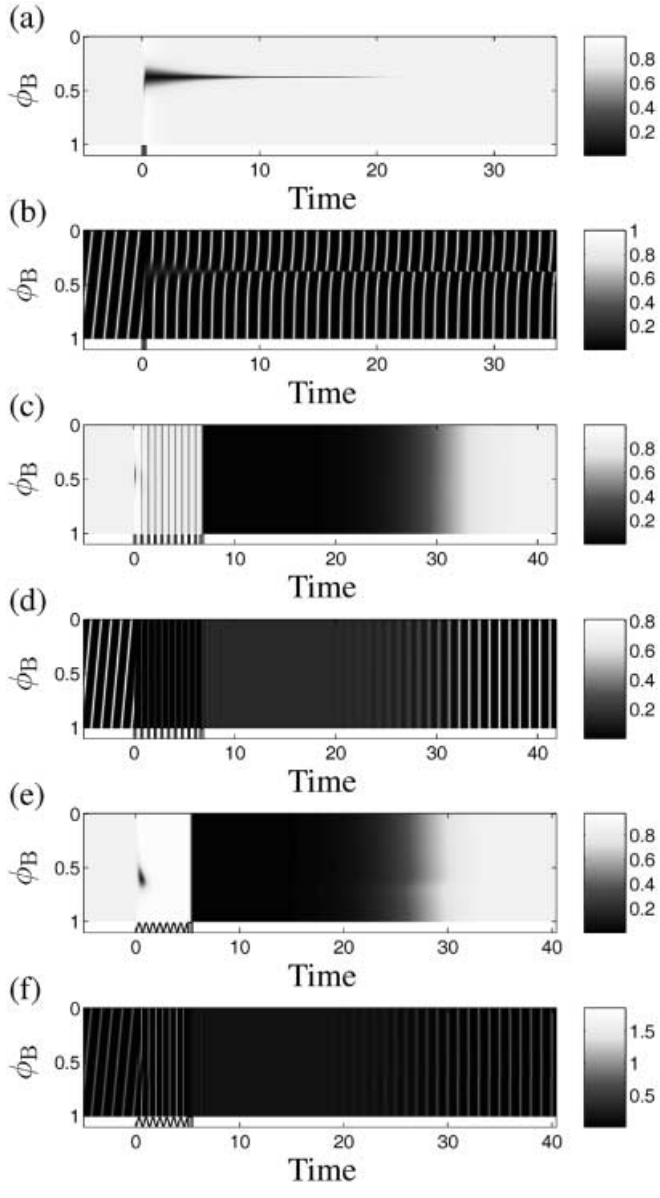

Fig. 2a–f. Time course of R, the amplitude of the order parameter defined by (6) (**a, c, e**), and the firing density $p(t) = n(0, t)$ (**b, d, f**) before, during, and after a *single pulse* (**a, b**), a *composite stimulus with pulsatile entrainment* (**c, d**), and a *composite stimulus with smooth entrainment* (**e, f**), where $\phi_B = \varphi_B/(2\pi)$ mod 1 is varied within one cycle. Stimulation starts at $t = 0$; for $t < 0$ the cluster is in the stable synchronized state. At the *bottom* of each plot single pulses are indicated by *bars*, whereas the time course of the strength of the sinusoidal entraining pulse is illustrated by plotting $\cos(\omega_s t)$, where ω_s is the entraining frequency from (8). In **a, b**; **c, d**; and **e, f** the parameters were as in Fig. 1b; Fig. 1d, e; and Fig. 1f, g; respectively

matter at which initial phase they are administered (Fig. 2c–f). To visualize the entrained firing in a pronounced way, in Fig. 2 the frequencies of the pulsatile and the smooth entrainment differ from the cluster's eigenfrequency Ω by 50% ($\omega_p = \omega_s = 1.5\,\Omega$). The smaller the frequency mismatch, $|\Omega - \omega_p|$ or $|\Omega - \omega_s|$, the more rapidly and easily a resetting entrainment is achieved. Thus, to save stimulation intensity (corresponding to the parameter I) and entrainment duration, in applications the entraining frequency (ω_p or ω_s) should be chosen close to the cluster's eigenfrequency Ω.

4.2 Block of resynchronization

The composite stimuli presented here desynchronize a cluster irrespective of its initial dynamic state and, in particular, irrespective of the extent of synchronization (i.e., the amplitude R from Eq. 6). For this reason the composite stimuli can be used to effectively block the cluster's resynchronization. To this end the same composite stimulus is administered to the cluster whenever it tends to resynchronize. This is illustrated in Fig. 3 by composite stimuli with pulsatile entrainment, and works analogously for composite stimuli with smooth entrainment. The larger the coupling strength K, the more often a composite stimulus has to be administered to prevent the cluster from resynchronization.

The amplitude of the synchronized firing in the entrained state crucially depends on the type of entrainment (pulsatile vs. smooth) and, furthermore, on the stimulation parameters. For the particular type of smooth entrainment considered here, the amplitude of the entrained firing is larger compared to the amplitude before stimulation (Fig. 2f). This would, of course, be a disadvantage in applications where the cluster has to be prevented from synchrony. By contrast, with a suitable choice of the stimulation parameters of the pulsatile

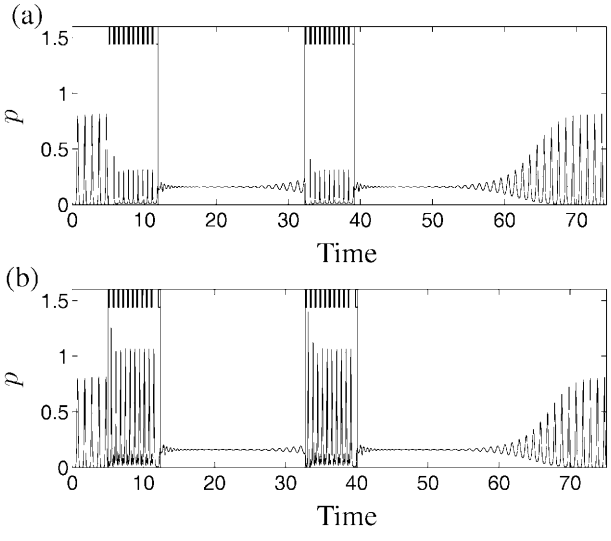

Fig. 3a,b. Time course of the firing density $p = n(0, t)$. **a** Two successively administered composite stimuli with pulsatile entrainment both with identical parameters (from Fig. 1d, e). The pulses of the pulse train are modelled by $S(\psi) = I\cos\psi$ with $I = 21$. The first composite stimulus desynchronizes the cluster, whereas the second blocks the resynchronization. **b** Two successively administered composite stimuli with pulsatile entrainment, where all parameters are as in **a** except for the intensity parameter I of the pulse train, which now has negative sign ($I = -21$), and the (longer) pause between resetting pulse train and desynchronizing single pulse. Note the difference in amplitude of the entrained firing. The begin and end of the composite stimuli are indicated by *vertical lines*; each single pulse is shown by a *shaded region* at the top of each panel

entrainment, the amplitude of the entrained firing is damped. For illustration, Fig. 3a shows the effect of a pulse train, where the pulses are modeled by $S(\psi) = I\cos\psi$ with $I = 21$, whereas Fig. 3b refers to a pulse train with $I = -21$. The amplitude of the entrained firing in Fig. 3b is clearly larger. To understand this difference we introduce a negative sign of the intensity parameter I in (1) and (3) by means of $S(\psi_j) = -I\cos\psi_j = I\cos(\psi_j + \gamma)$ with $I > 0$ and $\gamma = \pi$. The transformation $\phi_j = \psi_j + \gamma$ $(j = 1, \ldots, N)$ yields the Langevin equation $\dot{\phi}_j = \Omega + N^{-1}\sum_{l=1}^{N}\Gamma(\phi_j - \phi_l) + X(t)S(\phi_j) + F_j(t)$ which equals (1) and, hence, produces the same dynamics. The difference, however, is that now the single neuron fires whenever its phase equals $\phi^{\text{fire}} = \psi^{\text{fire}} + \gamma = \pi$, where $\psi^{\text{fire}} = 0$. As Z's orbit in the entrained state is not radially symmetric (Fig. 1d), the amplitude of the entrained firing is small when the neurons fire at phase zero (Fig. 3a), whereas it is large when the neurons fire at phase π (Fig. 3b). In general, we can minimize the amplitude of the entrained firing caused by a first-order stimulus $S(\psi) = I\cos(\psi + \gamma)$ (with $I > 0$) by means of an appropriate choice of γ, which here is equal to 0.18.

A resynchronization block cannot be achieved by repeatedly stimulating with the same single pulse. A single pulse appropriate for desynchronizing the fully synchronized cluster is too strong for a weakly synchronized cluster; instead of a desynchronization it causes a synchronization (Fig. 4). Therefore it is not possible to block the resynchronization by repeatedly administering the same single pulse used for desynchronizing the fully synchronized cluster. Even the following modified single-pulse method would not work. First, a desynchronization of the fully synchronized cluster is achieved with a stronger single pulse as shown in Fig. 4a. To block the resynchronization a weaker single pulse is then administered whenever the recovering amplitude of the order parameter R grows back to a small, fixed threshold R'. Note that for blocking the resynchronization, the same pulse (with the same intensity and duration) is repeatedly applied. As shown in Fig. 1b, desynchronizing the cluster means shifting Z into the origin of the Gaussian plane, so that after the pulse Z has to be as close to 0 as possible. For $Z = 0$ there is a phase singularity, and minimal variations of the stimulation parameters as well as noise – both inevitable in an experiment – let the phase of Z vary within $[0, 2\pi]$. For this reason the recovering Z may run along infinitely many spirals towards its stable limit cycle. Consequently, R' can be associated with infinitely many values of ϕ. Only one of these phase values is appropriate for a desynchronization. Generically, however, the weaker single pulse hits the cluster at a wrong initial phase, in this way synchronizing the cluster similarly as in Fig. 4.

5 Deep brain stimulation

In PD the standard, permanent high-frequency (>100 Hz) deep brain stimulation aims at suppressing pathological, synchonized activity in particular target areas such as the thalamic ventralis intermedius nucleus or the subthalamic nucleus (Benabid et al. 1991, 1994, 2000; Blond et al. 1992). Based on the results presented in this article I suggest a different therapy: demand-controlled deep brain stimulation with composite stimuli. For this, the deep brain electrode is used for both stimulation and registration of the feedback signal (the local field potential). A desynchronizing composite stimulus is administered only and whenever the pacemaker-like cluster becomes synchronized; put otherwise, whenever its LFP exceeds a critical value. The goal of this approach is to effectively block the resynchronization (Fig. 3a). As yet, no demand-controlled deep brain stimulation is used for the therapy of PD.

Already in the late 1950s it was shown that parkinsonian tremor is entrained by periodic deep brain pulsatile electrical stimulation of the pallidum at rates similar to the peripheral tremor frequency (Hassler et al. 1960). However, a desynchronizing composite stimulus has never been applied. There are two main reasons why demand-controlled stimulation technique should be less aggressive, and thus reduce side effects such as dysarthria and dysesthesia: (i) reducing the stimulating current reduces current spread and prevents stimulation of neighboring areas; and (ii) the demand-controlled method does not simply suppress the pathological firing,

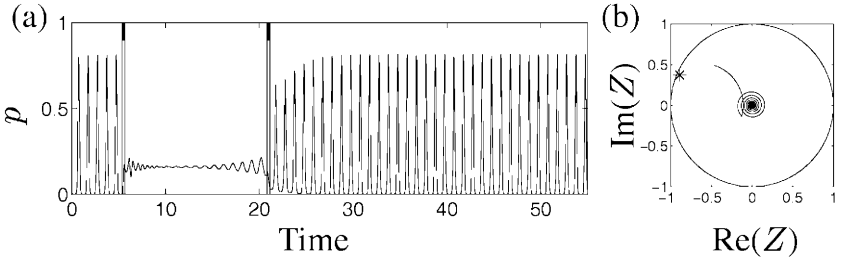

Fig. 4a,b. Two single pulses with identical pulse duration and intensity parameter I are successively administered at the same cluster phase φ. As in Fig. 1a and b, the single pulses are modeled by $S(\psi) = I\cos\psi$ with $I = 7$. The first single pulse hits the cluster in its fully synchronized state, whereas the second single pulse is administered to the weakly synchronized cluster. The firing density p is plotted in **a**, where the begin and end of pulses are indicated by *vertical lines* connected by a *shaded region*. The corresponding trajectory of the order parameter Z in the Gaussian plane between the end of the first and the end of the second single pulse is shown in **b**. After the first single pulse, Z starts spiraling towards its limit cycle. The second single pulse is too strong for the weakly synchronized cluster, and hence Z is shifted halfway to the attractor Z^{stat} from (7) (cf. Fig. 1a). Same network parameters as in Fig. 1

but rather it maintains an incoherent – in other words, nearly physiological (Nini et al. 1995) – firing, intersected by periods of entrained residual synchronous firing. For this application it is important to choose appropriate stimulation parameters in order to minimize the duration of the entrained epochs and, in particular, the amplitude of the entrained firing (Fig. 3). Of course, the impact of these epochs of low-amplitude residual synchrony on tremor generation has to be studied experimentally. For deep brain stimulation, a pulsatile soft reset has to be chosen instead of a sinusoidal soft reset, because extracellular sinusoidal stimulation at a frequency in the 5 Hz to 20 Hz range is not effective (Reilly 1998).

Before a desynchronizing composite stimulation can be performed, the critical stimulation parameters (the intensity of the single pulses, their duration, and the duration of the pauses in between) have to be determined in a series of test stimuli with a calibration procedure which corresponds to that of the double-pulse stimulation. Since the latter was explained in detail in Tass (2001c), here I merely mention that by means of phase-resetting curves, first, the quality of the reset has to be tested and, second, the pause between first and second stimulus as well as the intensity of the second stimulus are determined.

After the calibration the demand-controlled deep brain stimulation with composite stimuli starts. Always the same composite stimulus is applied to the same stimulation site as soon as the LFP exceeds its critical value. No further time-consuming online phase or frequency estimation or calibration has to be performed, provided the network parameters remain sufficiently stable (see Sect. 7).

5.1 Comparison of different stimulation techniques

The mechanism by which the standard, permanent high-frequency deep brain stimulation suppresses pathological rhythmic activity has not yet been clarified experimentally (Ashby and Rothwell 2000; Benabid et al. 2000; Benazzouz and Hallett 2000). Likewise, up to now results of experimental tests of the novel demand-controlled stimulation methods were not available. Therefore, in this section we compare the different stimulation techniques by applying them to model (1).

The demand-controlled methods aim at blocking the resynchronization (see Sect. 4.2). In modeling studies, three stimulation techniques turned out to be most suitable for demand-controlled deep brain stimulation (see Sect. 1): repeated administration (i) of a double pulse (Fig. 5a; Tass 2001a, c), (ii) of a high-frequency pulse train followed by a single pulse (Fig. 5b; Tass 2001b), or (iii) of a composite stimulus with pulsatile entrainment (Fig. 3a). In contrast, permanent high-frequency pulse-train stimulation applied to the model under consideration completely stops the neurons firing due to a high-frequency entrainment of the order parameter (Tass 2001b; Fig. 5c). As soon as the high-frequency stimulation ends, a particularly synchronous firing occurs in a rebound-like manner. Thus, to suppress the firing persistently, the periodic pulse-train stimulation has to be applied permanently.

We focus on the cumulative stimulation strength necessary either to maintain an uncorrelated firing (Figs. 3a, 5a, b) or to suppress the firing (Fig. 5c). The goal of this comparison is to provide an estimate of the energy consumption of the different demand-controlled stimulation techniques compared to the standard high-frequency stimulation. For the different stimulation techniques shown in Figs. 3a and 5, the stimuli were modeled by $S(\psi,t) = I(t)\cos\psi$ (cf. Eq. 3). $I(t)$ is an intensity parameter which is constant during a single pulse but may vary between pulses. Typically, the intensity parameter of a desynchronizing single pulse is smaller compared to that of a pulse belonging to a stronger, resetting stimulus. Since the effect of a stimulus on the single oscillator depends on the phase of the oscillator, we introduce

$$S_{\max}(t) = \max\{|S(\psi,t)|; \psi \in [0,2\pi]\} \tag{10}$$

in order to determine the maximal stimulation strength within a cycle $[0,2\pi]$ at time t. For $S(\psi,t) = I(t)\cos\psi$, we thus obtain $S_{\max}(t) = I(t)$.

The begin and end of a stimulus are denoted by τ_B and τ_E, respectively. For a desynchronizing stimulus, τ_B denotes the start of the resetting first single pulse (Fig. 5a) or the start of the resetting high- or low-frequency pulse train (Figs. 3a, 5b), whereas τ_E is the end of the directly following desynchronizing single pulse. Analogously, a long high-frequency pulse train starts at τ_B and ends at τ_E (Fig. 5c). The *mean cumulative stimulation strength* during stimulation is given by

$$S = \frac{1}{\tau_E - \tau_B} \int_{\tau_B}^{\tau_E} S_{\max}(t) X(t) \mathrm{d}t \tag{11}$$

with $X(t)$ from (4). In deep brain stimulation the intensity parameter $I(t)$ corresponds to a current flow through the brain tissue. Hence, S corresponds to the mean energy consumption during stimulation.

The permanent high-frequency stimulation suppresses the firing, so that the firing density vanishes: $p = 0$ (Fig. 5c). In contrast, the goal of the desynchronizing, demand-controlled stimulation techniques (Figs. 3a, 5a, b) is to maintain an uncorrelated firing by repeatedly administering a composite stimulus, so that the firing density p is kept close to the value belonging to a uniform desynchronization; i.e., close to $p = 1/(2\pi)$. Denoting the maximal value of the firing density in the stable synchronized state before stimulation by $p_{\max}$ (see Fig. 5b), the value belonging to an 80% suppression of $p_{\max}$ with respect to the uncorrelated firing is given by $p_{80\%} = 1/(2\pi) + [p_{\max} - 1/(2\pi)](1 - 80\%)$. With $p_{\max} = 0.81$, we obtain $p_{80\%} = 0.29$. To describe how long the stimuli shown in Figs. 3a and 5 keep the firing density below $p_{80\%}$, we introduce the following notations. Stimulation starts at time t_0, whereas $t_{80\%}$ is the timing point when the firing density p again exceeds $p_{80\%}$ (see Fig. 5b).

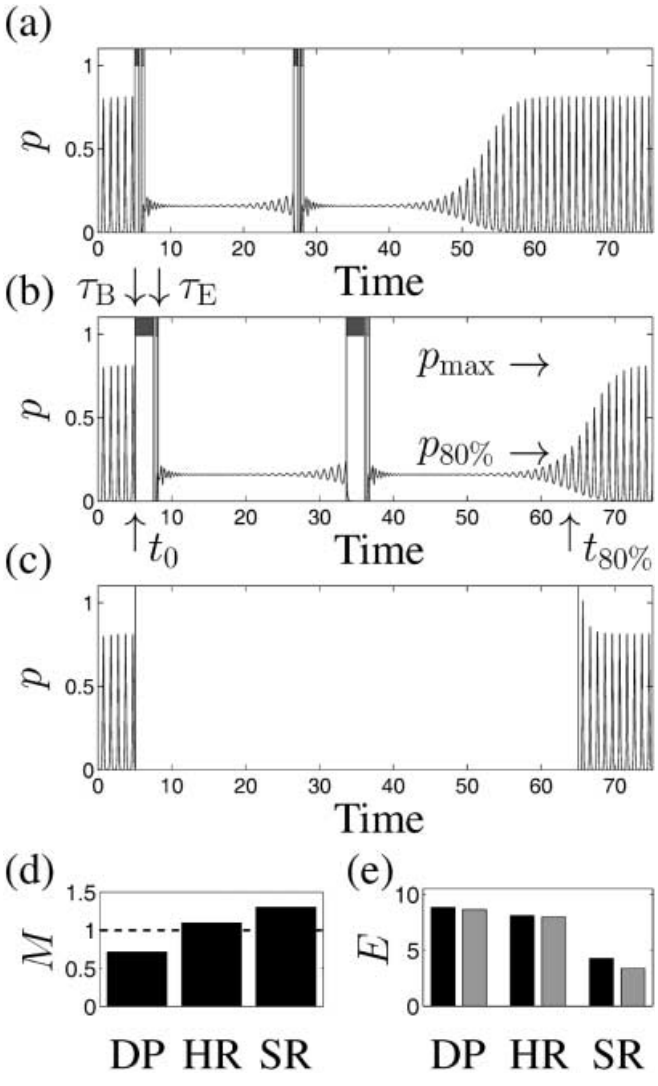

The *effective cumulative stimulation strength* necessary for an 80% suppression of the firing density is

$$S^{80\%} = \frac{1}{t_{80\%} - t_0} \int_{t_0}^{t_{80\%}} S_{\max}(t) X(t) \mathrm{d}t \ . \qquad (12)$$

For the composite stimulus with soft pulsatile entrainment (Fig. 3a), $t_{80\%} - t_0$ (the denominator of Eq. 12) has to be replaced by the duration $T_{80\%}$ during which p is actually below $p_{80\%}$. $T_{80\%}$ is smaller than $t_{80\%} - t_0$ if p exceeds $p_{80\%}$ during the pulsatile entrainment.

$S^{80\%}$ corresponds to the mean energy consumption necessary to keep the firing density below $p_{80\%}$. In the same way we determine $S^{x\%}$, the effective stimulation strength necessary for an $x\%$ suppression of the firing density. To compare the stimulation strength of the demand-controlled methods with the stimulation strength of the standard, high-frequency stimulation in model (1), we introduce the *ratios of the mean cumulative stimulation strengths* during stimulation as

$$M_{\mathrm{DP}} = \frac{S_{\mathrm{ST}}}{S_{\mathrm{DP}}}, \ M_{\mathrm{HF}} = \frac{S_{\mathrm{ST}}}{S_{\mathrm{HF}}}, \ M_{\mathrm{SR}} = \frac{S_{\mathrm{ST}}}{S_{\mathrm{SR}}} \ , \qquad (13)$$

◀

Fig. 5a–d. Comparison between different demand-controlled stimulation techniques and the standard method, where all stimuli are applied to the same network as in Fig. 1. **a** Two successively administered double pulses. The begin and end of a single pulse are denoted by vertical lines connected by a shaded region. **b** The same high-frequency pulse train followed by a single pulse is applied twice. τ_B and τ_E denote the begin and end of a (composite) stimulus (*downward arrows*). $p_{\max}$ is the maximal value of the firing density in the stable synchronized state, whereas $p_{80\%} = 1/(2\pi) + [p_{\max} - 1/(2\pi)](1 - 80\%)$ is the 80% suppression level compared to the uncorrelated firing $p = 1/(2\pi)$ (*horizontal arrows*). Stimulation keeps p below $p_{80\%}$ between times t_0 and $t_{80\%}$ (*upward arrows*). *Vertical lines* connected by a *shaded region* indicate the begin and end of a high-frequency pulse train or of a single pulse. **c** A permanent high-frequency pulse train suppresses the collective firing. Directly after stimulation the cluster restarts in a rebound-like manner. *Vertical lines* indicate the begin and end of the high-frequency stimulation. The ratios of the mean cumulative stimulation strengths during stimulation (M_{DP}, M_{HF}, and M_{SR}) from (13) are shown in **d**. During stimulus administration, our stimulation technique is milder than the standard high-frequency stimulation provided its value of M is greater than 1. The ratios of the effective cumulative stimulation strengths necessary for a 70% suppression ($E_{\mathrm{DP}}^{70\%}$, $E_{\mathrm{HF}}^{70\%}$, and $E_{\mathrm{SR}}^{70\%}$, in *black*) and an 80% suppression ($E_{\mathrm{DP}}^{80\%}$, $E_{\mathrm{HF}}^{80\%}$, and $E_{\mathrm{SR}}^{80\%}$, in *gray*) of the firing density as defined by (14) are displayed in **e** (*DP*, double pulse; *HR*, high-frequency pulse train; *SR* soft reset). Our stimulation technique is more efficient than the standard high-frequency stimulation provided its value of E is greater than 1. Stimulation parameters were as follows: In **a**–**c**, all stimuli are modeled by $S(\psi) = I\cos\psi$. Intensity parameter I: **a** $I = 21$ for the first and $I = 7$ for the second pulse; **b** $I = 21$ for the high-frequency pulse train and $I = 7$ for the subsequent desynchronizing pulse; **c** $I = 21$ for the high-frequency pulse train. Pulse durations: **a** duration of the first pulse = 0.5 and of the second pulse = 0.31; **b** duration of the pulses in the pulse train = 0.02 with pauses of length = 0.03 in between, duration of the desynchronizing single pulse = 0.31; **c** same pulse train as in **b**, but without the subsequent desynchronizing single pulse

where DP stands for the double pulse from Fig. 5a, and HF denotes the high-frequency pulse train followed by a single pulse from Fig. 5b. SR ("soft reset") stands for the composite stimulus with soft pulsatile entrainment from Fig. 3a, and ST is the abbreviation for the standard high-frequency stimulation from Fig. 5c. S_{DP}, S_{HF}, S_{SR}, and S_{ST} are the mean cumulative stimulation strength of DP, HF, SR, and ST, respectively. In analogy to (13) we introduce the *ratios of the effective cumulative stimulation strengths* necessary for an 80% suppression of the firing density as

$$E_{\mathrm{DP}}^{80\%} = \frac{S_{\mathrm{ST}}^{80\%}}{S_{\mathrm{DP}}^{80\%}}, \ E_{\mathrm{HF}}^{80\%} = \frac{S_{\mathrm{ST}}^{80\%}}{S_{\mathrm{HF}}^{80\%}}, \ E_{\mathrm{SR}}^{80\%} = \frac{S_{\mathrm{ST}}^{80\%}}{S_{\mathrm{SR}}^{80\%}} \ . \qquad (14)$$

Figure 5d and e displays the ratios defined by (13) and (14) which were determined for the simulations shown in Figs. 3a and 5a–c. A 100% suppression would not be a realistic goal for experimental applications. Accordingly, the comparison between the different stimulation techniques is performed for reasonable suppression levels. It turns out that the demand-controlled methods are considerably more effective than the standard high-frequency stimulation: $E_{\mathrm{DP}}^{80\%} = 8.63$, $E_{\mathrm{HF}}^{80\%} = 7.97$, $E_{\mathrm{SR}}^{80\%} = 3.38$, and $E_{\mathrm{DP}}^{70\%} = 8.82$, $E_{\mathrm{HF}}^{70\%} = 8.11$, $E_{\mathrm{SR}}^{70\%} = 4.25$ (Fig. 5e). The difference between the 70%

and 80% suppression levels is largest for the SR method, since during the pulsatile entrainment the peaks of p are larger than $p_{80\%}$ and smaller than $p_{70\%}$, so that $T_{80\%}$ is smaller than $t_{80\%} - t_0$ (see above).

Especially for the demand-controlled techniques, the effective cumulative stimulation strengths $S^{70\%}$ and $S^{80\%}$ from (12) crucially depend on the time necessary to resynchronize, and thus on the ratio between coupling strength and noise amplitude. The cluster of oscillators resynchronizes provided its coupling K exceeds the critical value $K_{\text{crit}} = D = 0.4$ (Tass 1999). No experimental data are available that would allow estimation of appropriate values of K. Therefore, throughout the present study K was chosen to be clearly supercritical, namely equal to 1. This means that the cluster resynchronizes rather rapidly, which is more challenging for the demand-controlled techniques. For K closer to K_{crit}, the ratios from (14) are even larger than those obtained for $K = 1$. In other words, the weaker the coupling the smaller is the energy consumption of the demand-controlled methods.

From Fig. 5e it follows that the double pulse is most effective. However, from Fig. 5d we see that the double pulse is the only stimulation technique with a mean cumulative stimulation strength during stimulation that is greater than that of the standard high-frequency stimulation ($M_{\text{DP}} = 0.72$, $M_{\text{HF}} = 1.10$, $M_{\text{SR}} = 1.30$; Fig. 5d). This means that the high-frequency pulse train followed by a single pulse, and the composite stimulus with soft pulsatile entrainment are the only methods which are both more efficient and milder compared to the standard high-frequency stimulation. Concerning the energy consumption, the high-frequency pulse train followed by a single pulse is most advantageous. However, avoiding a hard reset may be beneficial for clinical applications, as discussed in Sect. 7.

6 Sensory manipulation of visual binding

Neuronal oscillatory activity in cat (Rager and Singer 1998) and human (Herrmann 2001) visual cortex can be entrained by means of a flickering visual stimulus; i.e., a periodic train of visual single-pulse stimuli, which has a frequency ω_{p} (see Sect. 3.2) that is close to resonance frequencies such as 10 Hz, 20 Hz, 40 Hz, and 80 Hz. This leads to a resonance-like increase of the amplitude of the neuronal activity. Resonance phenomena of this kind are not restricted to simple light flashes. They are found even for complex visual stimuli such as Kanizsa-like patterns (i.e., arrangements of particularly formed angles mixed with randomly distributed angles): cerebral processing of Kanisza-like visual stimuli is much faster when they flicker at the resonance frequency (40 Hz) than at other frequencies (Elliot and Müller 1998). Furthermore, a flicker frequency close to 40 Hz gives rise to reduced latencies of stimulus-evoked electroencephalographic gamma responses (Elliot et al. 2000).

Instead of enhancing gamma activity by entrainment, I suggest an opposite manipulation, which is to desynchronize gamma activity by means of the combined stimulation technique presented in this article, where ω_{p} is close to 40 Hz. In a first step this should be done with simple flickering light flashes, where the duration of a light flash corresponds to the duration of a single pulse of the composite stimulus from Fig. 3, and the intensity of the light flash corresponds to the intensity parameter I. To investigate visual binding, more complex flickering stimuli such as Kanisza patterns have to be used, where – similar to the light flashes – the timing and intensity sequence of the Kanisza patterns realizes a desynchronizing composite stimulus. One could also try to replace the flickering soft reset (with a pulse train) by a smooth soft reset using a sinusoidal visual stimulus with frequency ω_{s} from (8) close to 40 Hz. The motivation behind this approach is to try to block the gamma activity at least temporarily, as shown in Fig. 3, and to measure the consequences both with respect to electrophysiology and psychophysiology: the impact on brain activity can then be assessed with electroencephalography and magnetoencephalography in humans, or with electrical recordings in animals, whereas psychophysical testing provides estimates of the velocity of cerebral information processing.

To compare the functional role of gamma activity with that of other brain rhythms during binding, one should perform the desynchronizing visual stimulation with visual patterns that both essentially require and do not require visual binding. To illustrate this approach let us consider an experiment where the composite visual stimulation is separately performed with a complete triangle (Fig. 6a) as well as with an incomplete triangle (Fig. 6b). To perceive the latter as a whole (i.e., as an unbroken triangle), all different short lines of the triangular arrangement have to be linked up correctly by the visual system (see Singer 1989). Accordingly, for recognizing Fig. 6b as a triangle, visual binding is essential. The experiment consists of two different parts:

1. *Entrainment by constant flickering*. It has to be tested whether a constantly flickering, periodic stimulation entrains activity in visual cortical areas. The entrainment has to be performed for both visual stimuli in Fig. 6 separately. This part of the experiment corresponds to the entrainment experiments mentioned above (i.e., Rager and Singer 1998; Elliot et al. 2000;

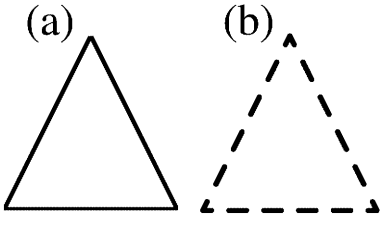

Fig. 6a,b. The complete (**a**) and incomplete (**b**) triangles used for desynchronizing visual composite stimulation, as explained in the text. The incomplete triangle consists of an arrangement of short lines which have to be bound by the visual system in order to be perceived as an intact triangle

Herrmann 2001). For this, the flickering frequency has to be varied within a large range of frequencies, e.g., from 1 Hz to 100 Hz. The goal of this part is to identify optimal entrainment frequencies for the two visual stimuli from Fig. 6. A robust entrainment is necessary for a soft reset.

2. *Desynchronization with composite stimuli at optimal entrainment frequencies*. The next step is to perform a composite visual stimulation with the two different stimuli in Fig. 6 separately. For both visual stimuli it has to be tested whether a desynchronization can be achieved for all optimal entrainment frequencies. To this end the frequency of a soft reset has to be identical to an optimal entrainment frequency. The goal of this part of the experiment is to selectively desynchronize oscillatory brain activity and to study the functional (i.e., electrophysiological and especially psychophysiological) consequences.

Comparing the entrainment and desynchronization behavior of the two different stimuli from Fig. 6 may reveal brain rhythms which are exclusively necessary for visual binding. For example, let us assume that activity in the 40-Hz range can be desynchronized by means of composite stimulation with both stimuli in Fig. 6. If the perception of the complete triangle (Fig. 6a) would not be affected by the desynchronization, whereas the perception of the incomplete triangle (Fig. 6b) would strongly be retarded or weakened, the functional relevance of gamma activity for visual binding could be demonstrated.

In this way it can be verified whether gamma activity can be blocked with composite visual stimuli, and how that correlates with function, e.g., in terms of an increase of response latencies or an increase of error rates. Instead of the visual patterns shown in Fig. 6, a different pair of patterns can alternatively be chosen. The main point is that perception of one of the stimuli requires visual binding, whereas perception of the other one does not require visual binding.

The critical flicker fusion frequency (CFF) is the minimal frequency at which a visual stimulus is perceived in a fused, steady way (Kelly 1972): for scotopic vision, maximal values of CFF lie in the 22–25 Hz range, whereas for photopic vison the CFF crucially depends on stimulus parameters such as light intensity and size. The interruption of the visual stimulation occurring after each composite stimulus (Fig. 3) may lead to a discontinuous, nonfused perception of the stimulus. To compare effects of the visual patterns from Fig. 6 presented either flickering at 40 Hz or as a composite stimulus (Fig. 3), one should exclude effects that are related to discontinuous perception caused by a stimulus presented at a frequency which is repeatedly lower than the CFF. For this, one might alternatively modify the visual stimulation by replacing the periods without any visual stimulation by a stimulation with the same visual stimulus periodically flickering at a different frequency ω_f. This stimulation should be sufficiently detuned so that it does not strongly entrain the gamma activity and, furthermore, ω_f should be greater than the CFF. The timing sequence of the visual stimulation would then be as follows. A composite stimulus with a soft reset with frequency ω_p is performed to desynchronize activity in the frequency range related to ω_p. Directly after the composite stimulus, the same visual pattern is administered with a flicker frequency ω_f, where $\omega_f \neq \omega_p$. As soon as the amplitude of the activity around ω_p increases again, the next composite stimulus is administered (again, with the same visual stimulus), which is then followed by the ω_f flicker, and so on.

7 Discussion

Two composite stimulation techniques are presented in this article which make it possible to effectively desynchronize a cluster of interacting phase oscillators without making use of any strong stimulus. This is particularly important for applications in biology and medicine, since previously designed methods for effective desynchronization (Tass 1999, 2000, 2001a–c) essentially rely on a hard reset that requires a strong, abruptly resetting stimulus. A hard reset is achieved within less than one period of the collective oscillation by means of a strong single pulse (Tass 2001a, c) or a high-frequency pulse train (with an entraining frequency that is approximately 20 times larger than the cluster's eigenfrequency; Tass 2001b). Such a maneuver, however, might be too strong and might even injure neuronal tissue (or other biological systems). A way to avoid this risk is provided by the novel composite stimulation methods which use a soft reset: during a pulsatile or a smooth periodic entrainment at a rate close to the cluster's eigenfrequency, the influence of the initial dynamic state at the beginning of the periodic stimulation disappears, while the collective oscillation runs through several periods. After the soft reset a moderate single pulse follows with a constant time delay, which desynchronizes the cluster by hitting it in a vulnerable state.

While the desynchronizing effect of a composite stimulus does not depend on the particular type of the entraining stimulus, the pattern – and especially the amplitude – of the entrained firing crucially do. No matter whether a pulsatile entrainment or a smooth entrainment is used, the desynchronization obtained with the composite stimulus is equally good (Fig. 2c–f). By contrast, the amplitude of the entrained firing may be smaller (Fig. 3a) or larger (Figs. 2f, 3b) compared to the firing before stimulation. The choice of the most appropriate type of entrainment depends on the application and, of course, on possible experimental restrictions. For instance, sinusoidal extracellular stimulation of neural tissue at frequencies in the 5 Hz to 20 Hz range is not effective (Reilly 1998). Thus, for extracellular deep brain stimulation, a pulsatile entrainment has to be used instead of a sinusoidal entrainment. Furthermore, it has to be tested whether a variation of the stimulation parameter γ in $S(\psi) = I\cos(\psi + \gamma)$ can be performed experimentally (see Sect. 4.2). If so, an appropriate value for γ has to be chosen in order to minimize the amplitude

of the entrained firing (Fig. 3). For applications it is also important that a soft reset is not restricted to a (pulsatile or smooth) 1:1 entrainment. Rather, one can also use a (pulsatile or smooth) n:m entrainment, where n and m are small integers, and n:m is the ratio between the stimulation frequency and the mean frequency of the rhythm which is to be desynchronized. Hence, in an experimental application where 1:1 entrainment is not effective, different n:m entrainment ratios should be tested.

Since rhythmic activity abounds in physiology, the presented stimulation techniques may find various applications where rhythms have to be desynchronized for scientific or therapeutic purposes. Two applications are suggested: demand-controlled deep brain stimulation (Sect. 5) and sensory manipulation of gamma activity (Sect. 6). Both applications are very promising because pulsatile entrainment has already been demonstrated experimentally for deep brain stimulation in PD (Hassler et al. 1960) as well as for visual stimulation of gamma activity in cat (Rager and Singer 1998) and human (Herrmann 2001) visual cortex. However, up to now composite stimulation for desynchronization has never been applied. Likewise, the novel methods can also be applied to desynchronize other brain rhythms such as alpha or beta rhythm which both can also be entrained by flickering stimuli (Rager and Singer 1998; Herrmann 2001).

Smoothly moving stimuli produce sustained gamma oscillations in different visual cortical areas that are synchronized in phase, both in anesthetized cat (Eckhorn et al. 1988; Gray and Singer 1989) and awake monkey (Kreiter and Singer 1992; Eckhorn et al. 1993). Perturbing the smooth visual stimulation with qualitatively different stimuli – namely with intermingled sudden random accelerations of the grating – suppresses the gamma oscillations, where with increasing amplitude of the random perturbations the related evoked fast responses increase, whereas the amplitude of gamma oscillations gradually decreases (Kruse and Eckhorn 1996). The suppression of gamma oscillations is, hence, intimately related to a switching between different percepts (Kruse and Eckhorn 1996). Compared to the approach used by Kruse and Eckhorn (1996), the desynchronizing composite visual stimulation technique in Sect. 6 would enable investigation of the relationship between a single percept and the extent of gamma oscillations without making use of additional stimuli related to different percepts, i.e., without switching between different percepts.

For applications of the novel stimulation techniques, it has to be taken into account that higher-order terms of the stimulus (3), such as $S(\psi) = I\cos(m\psi)$ with $m > 1$, may cause an excitation of higher-order frequency components with an average number density $n(\psi, t)$, which shows up as a higher-frequency, pronounced early response of the cluster's firing directly after the stimulus. The mechanism behind this unwanted effect has been studied in detail in the context of single-pulse (Tass 1999) and double-pulse stimulation (Tass 2001c). There it was explained how to avoid this phenomenon, namely by suitably modifying the stimulation mechanism in a way that it damps higher-order modes. The impact of a stimulus on the different frequency components is reliably assessed by extracting these components out of the experimetal data by means of band-pass filtering and Hilbert transformation (Tass 1999).

Instead of the suggested demand-controlled stimulation mode (Sects. 5, 6), one can also choose a technically more straightforward type of stimulation, without feedback control: by simply delivering a composite stimulus periodically, the unwanted synchronized firing can also be kept down. In this case the period of stimulus administration has to be smaller compared to the experimentally determined minimal resynchronization time. Since it is technically much easier to realize, the periodic stimulation mode might be a relevant alternative for the sensory stimulation of gamma activity (Sect. 6). For deep brain stimulation (Sect. 5), however, demand-controlled stimulation is clearly superior. On the one hand stimulation has to be avoided during silent periods, which means when there is no pacemaker-like pathological rhythm. Keeping the stimulation current at a minimum improves the battery life, so that the surgical replacement of the generator and its battery could occur less frequently. Furthermore, minimizing the stimulation current reduces the possibility of adaptive reactions of the stimulated network. Adaptation of the network and, in general, variations of network parameters may spoil the stimulation outcome. Accordingly, monitoring the activity of the target area is required to detect a diminution of the stimulus action that might evolve on a long timescale. In such a case, the stimulator has to be recalibrated in order to maintain a strong desynchronization.

Based on model (1), the energy consumption of the demand-controlled stimulation techniques was theoretically estimated and compared to that of the standard high-frequency stimulation (Sect. 5.1). The demand-controlled techniques are clearly superior, even in the case of rather strong coupling which gives rise to a rapid resynchronization. However, this comparison cannot be reduced to evaluating only one parameter, namely the energy consumption. Since there are neuronal populations in the target areas used for deep brain stimulation which are not primarily part of motor loops, other brain functions such as cognition are also affected by deep brain stimulation (see Saint-Cyr et al. 2000). As yet, effects of this kind cannot be treated sufficiently by means of network simulations; rather, a clinical evaluation of the different demand-controlled stimulation techniques is inevitable. This can only be achieved by applying the novel techniques in patients and measuring the benefit with respect to an attenuation of motor as well as nonmotor symptoms.

According to theoretical studies there are several effective desynchronizing stimulation techniques. Let me therefore sketch how an experimentalist selects the appropriate one for a given application. First, the experimentalist has to check whether a hard reset can, in principle, be obtained with a compatible stimulation intensity. To this end, in a series of test stimuli the ex-

perimentalist has to study whether the response of the stimulated cluster is independent of its dynamic state at the beginning of the stimulation. This criterion was explained in Tass (2001a–c).

If a hard reset can be applied, the experimentalist can choose between three different variants of double-pulse stimulation (Tass 2001a, c) on the one hand, and a combined high-frequency pulse train, single-pulse stimulation (Tass 2001b) on the other hand. The applicability of the different double-pulse methods is compared in Tass (2001c). The resetting effect of a strong single pulse compared to that of a high-frequency pulse train (e.g., when using the same stimulating current) is practically the same (Tass 2001b). Thus, for several applications the combined high-frequency pulse trainsingle-pulse stimulation may be milder.

If a hard reset is not feasible, the experimentalist has to test whether a soft reset can be performed. To this end the experimentalist measures phase and amplitude of the order parameter Z from (6), and of higher-order frequency modes before and after entraining stimulation or – if there are no stimulus artifacts – continuously during stimulation by means of the mean mutual distance $d(t)$ from (9). How to reconstruct the order parameter and higher-order modes from the experimental data with band-pass filtering and Hilbert transformation is explained in Tass (1999). At the end of the entraining, periodic stimulation phase and amplitude of the order parameter and the higher-order modes have to be identical, so that they no longer depend on the initial dynamic conditions. The intensity and number of entrainment periods have to be large enough to fulfill this criterion.

If both a hard and a soft reset are possible, the experimentalist can choose which to use whilst taking into account that a soft reset will often be milder. However, the residual entrained firing during the soft reset may spoil the functional outcome of the resynchronization block (Fig. 3). Furthermore, the shorter the reset the less probable fluctuations or unforeseen external influences interfere with the desynchronizing effect of the stimulus.

The composite stimulation techniques presented in this article also work perfectly when applied to noisy cluster states – the so-called noisy m-cluster states. These are complex synchronized states, where a large cluster of oscillators breaks into m different subclusters, in each of which all oscillators have (nearly) the same phase ($m = 2, 3, \ldots$; Golomb et al. 1992). Noisy cluster states are caused by coupling terms of higher order such as $\Gamma(x) = -K_m \sin(mx)$ (with $K_m > 0$). An m-cluster state emerges when K_m exceeds its critical value mD (Tass 1999). For example, two clusters synchronized in antiphase form a two-cluster state. The order parameter of an m-cluster state is $Z_m(t) = \int_0^{2\pi} n(\psi, t) \exp(im\psi) \mathrm{d}\psi$. Z_m runs on a limit cycle similar to Z's limit cycle described in Sect. 2.2, and $|Z_m|$ quantifies the extent of synchronization of the m-cluster state, where $0 \leq |Z_m| \leq 1$ for all times t. To desynchronize Z_m most effectively (as shown in Fig. 1d–g), the stimulus should contain terms of mth order such as $S(\psi) = I \cos(m\psi)$. Note that composite stimuli are equally effective if the coupling contains cosine terms.

Although model (1) is rather simple, it nevertheless reproduces some dynamical features observed in experiments with peripheral stimulation or repetitive deep brain stimulation (for a detailed discussion, see Tass 1999). Thus, one may consider the present model also as a suitable starting point for more microscopic modeling. Accordingly, the impact of bipolar pulses as well as spatially distributed synaptic coupling strengths, eigenfrequencies, and stimulation strengths on the stimulation effects is now being studied by us in networks of phase oscillators and Hodgkin-Huxley neurons. The results will be presented in the near future. Concerning the influence of the spatial pattern of the synaptic coupling strengths, it is important to stress that the basic desynchronizing mechanism shown in Fig. 1b holds as well for an ensemble of noninteracting phase oscillators (Tass 1996a, 1999). In other words, if the stimulation strength is sufficiently large compared to the coupling strength, the desynchronizing effect does not depend on the coupling pattern (provided the stimulator is appropriately calibrated). By contrast, the dynamics following the desynchronization crucially does. While the interacting cluster resynchronizes (Fig. 2), the noninteracting ensemble remains incoherent (Tass 1996a, 1999).

Acknowledgements. I am grateful to Gereon R. Fink and Peter H. Weiss for our fruitful discussions. This study was supported by the German–Israeli Foundation for Scientific Research and Development (grant no. 667/00).

References

Alberts WW, Wright EJ, Feinstein B (1969) Cortical potentials and parkinsonian tremor. Nature 221: 670–672

Ashby P, Rothwell JC (2000) Neurophysiologic aspects of deep brain stimulation. Neurology 55[Suppl 6]: S17–S20

Benabid AL, Pollak P, Gervason C, Hoffmann D, Gao DM, Hommel M, Perret JE, de Rougemont J (1991) Long-term suppression of tremor by chronic stimulation of the ventral intermediate thalamic nucleus. Lancet 337: 403–406

Benabid AL, Pollak P, Gross C, Hoffmann D, Benazzouz A, Gao DM, Laurent A, Gentil M, Perret J (1994) Acute and long-term effects of subthalamic nucleus stimulation in Parkinson's disease. Stereotact Funct Neurosurg 62: 76–84

Benabid AL, Koudsié A, Benazzouz A, Fraix V, Ashraf A, Le Bas JF, Chabardes S, Pollak P (2000) Subthalamic stimulation for Parkinson's disease. Arch Med Res 31: 282–289

Benazzouz A, Hallett M (2000) Mechanism of action of deep brain stimulation. Neurology 55[Suppl 6]: S13–S16

Bergman H, Wichmann T, Karmon B, DeLong MR (1994) The primate subthalamic nucleus. II. Neuronal activity in the MPTP model of parkinsonism. J Neurophysiol 72: 507–520

Best EN (1979) Null space in the Hodgkin–Huxley equations: a critical test. Biophys J 27: 87–104

Blond S, Caparros-Lefebvre D, Parker F, Assaker R, Petit H, Guieu JD, Christiaens JL (1992) Control of tremor and involuntary movement disorders by chronic stereotactic stimulation of the ventral intermediate thalamic nucleus. J Neurosurg 77: 62–68

Eckhorn R, Bauer R, Jordan W, Brosch M, Kruse W, Munk M, Reitboeck HJ (1988) Coherent oscillations: a mechanism of feature linking in the visual cortex? Biol Cybern 60: 121–130

Eckhorn R, Frien A, Bauer R, Woelbern T, Kehr H (1993) High frequency 60–90 Hz oscillations in primary visual cortex of awake monkey. Neuroreport 4: 243–246

Elble RJ, Koller WC (1990) Tremor. John Hopkins University Press, Baltimore, Md.

Elliot MA, Müller HJ (1998) Synchronous information presented in 40-Hz flicker enhances visual feature binding. Psychol Sci 9: 277–283

Elliot MA, Herrmann CS, Mecklinger A, Müller H (2000) The loci of oscillatory visual-object priming: a combined electroencephalographic and reaction-time study. Int J Psychophysiol 38: 225–242

Ermentrout GB, Kopell N (1991) Multiple pulse interactions and averaging in systems of coupled neural oscillators. J Math Biol 29: 195–217

Ghose GM, Freeman RD (1992) Oscillatory discharge in the visual system:does it have a functional role? J Neurophysiol 68: 1558–1574

Ghose GM, Maunsell J (1999) Specialized representations in visual cortex: a role for binding? Neuron 24: 79–85

Golomb D, Hansel D, Shraiman B, Sompolinsky H (1992) Clustering in globally coupled phase oscillators. Phys Rev A 45: 3516–3530

Grannan ER, Kleinfeld D, Sompolinsky H (1993) Stimulus-dependent synchronization of neuronal assemblies. Neural Comput 4: 550–569

Gray CM, Singer W (1989) Stimulus-specific neuronal oscillations in orientation columns of cat visual cortex. Proc Natl Acad Sci USA 86: 1698–1702

Gray CM, Engel AK, König P, Singer W (1992) Synchronization of oscillatory neuronal responses in cat striate cortex: temporal properties. Vis Neurosci 8: 337–347

Guttman R, Lewis S, Rinzel J (1980) Control of repetitive firing in squid axon membrane as a model for a neuroneoscillator. J Physiol (Lond) 305: 377–395

Haken H (1983) Advanced synergetics. Springer, Berlin Heidelberg New York

Hansel D, Mato G, Meunier C (1993) Phase dynamics of weakly coupled Hodgkin–Huxley neurons. Europhys Lett 23: 367–372

Hassler R, Riechert T, Mundinger F, Umbach W, Ganglberger JA (1960) Physiological observations in stereotaxic operations in extrapyramidal motor disturbances. Brain 83: 337–350

Herrmann CS (2001) Human EEG responses to 1–100 Hz flicker: resonance phenomena in visual cortex and their potential correlation to cognitive phenomena. Exp Brain Res 137: 346–353

Kelly DH (1972) Flicker. In: Jameson D, Hurvich LM (eds) Handbook of sensory physiology and visual psychophysics, vol VII/4. Springer, Berlin Heidelberg New York, pp 271–302

Kreiter AK, Singer W (1992) Oscillatory neuronal responses in the visual cortex of the awake macaque monkey. Eur J Neurosci 4: 369–375

Kruse W, Eckhorn R (1996) Inhibition of sustained gamma oscillations (35–80 Hz) by fast transient responses in cat visual cortex. Proc Natl Acad Sci USA 93: 6112–6117

Kuramoto Y (1984) Chemical oscillations, waves, and turbulence. Springer, Berlin Heidelberg New York

Lamarre Y, de Montigny C, Dumont M, Weiss M (1971) Harmaline-induced rhythmic activity of cerebellar and lower brain stem neurons. Brain Res 32: 246–250

Lenz FA, Kwan HC, Martin RL, Tasker RR, Dostrovsky JO, Lenz YE (1994) Single unit analysis of the human ventral thalamic nuclear group. Tremor-related activity in functionally identified cells. Brain 117: 531–543

Llinás R, Jahnsen H (1982) Electrophysiology of mammalian thalamic neurons in vitro. Nature 297: 406–408

Nini A, Feingold A, Slovin H, Bergman H (1995) Neurons in the globus pallidus do not show correlated activity in the normal monkey, but phase-locked oscillations appear in the MPTP model of parkinsonism. J Neurophysiol 74: 1800–1805

Pare D, Curro'Dossi R, Steriade M (1990) Neuronal basis of the parkinsonian resting tremor: a hypothesis and its implications for treatment. Neuroscience 35: 217–226

Rager G, Singer W (1998) The response of cat visual cortex to flicker stimuli of variable frequency. Eur J Neurol 10: 1856–1877

Reilly JP (1998) Applied bioelectricity – from electrical stimulation to electropathology. Springer, Berlin Heidelberg New York

Riesenhuber M, Poggio T (1999) Are cortical models really bound by the ''binding problem''? Neuron 24: 87–93

Saint-Cyr JA, Trepanier LL, Kumar R, Lozano AM, Lang AE (2000) Neuropsychological consequences of chronic bilateral stimulation of the subthalamic nucleus in Parkinson's disease. Brain 123: 2091–2108

Singer W (1989) Search for coherence: a basic principle of cortical self-organization. Concepts Neurosci 1: 1–26

Stoney SD Jr, Thompson WD, Asanuma H (1968) Excitation of pyramidal tract cells by intracortical microstimulation: effective treatment of stimulating current. J Neurophysiol 31: 659–669

Tass PA (1996a) Resetting biological oscillators – a stochastic approach. J Biol Phys 22: 27–64

Tass PA (1996b) Phase resetting associated with changes of burst shape. J Biol Phys 22: 125–155

Tass PA, Rosenblum MG, Weule J, Kurths J, Pikovsky A, Volkmann J, Schnitzler A, Freund H-J (1998) Detection of *n*:*m* phase locking from noisy data: application to magnetoencephalography. Phys Rev Lett 81: 3291–3294

Tass PA (1999) Phase resetting in medicine and biology – stochastic modelling and data analysis. Springer, Berlin Heidelberg New York

Tass PA (2000) Stochastic phase resetting: a theory for deep brain stimulation. Prog Theor Phys Suppl (Kyoto) 139: 301–313

Tass PA (2001a) Effective desynchronization by means of double-pulse phase resetting. Europhys Lett 53(1): 15–21

Tass PA (2001b) Effective desynchronization with a resetting pulse-train followed by a single pulse. Europhys Lett 55: 171–177

Tass PA (2001c) Desynchronizing double-pulse phase resetting and application to deep brain stimulation. Biol Cybern 85: 343–354

Tass PA (2002) Effective desynchronization with a stimulation technique based on soft phase resetting. Europhys Lett 57: 164–170

Volkmann J, Joliot M, Mogilner A, Ioannides AA, Lado F, Fazzini E, Ribary U, Llinás R (1996) Central motor loop oscillations in parkinsonian resting tremor revealed by magnetoencephalography. Neurology 46: 1359–1370

Winfree AT (1980) The geometry of biological time. Springer, Berlin Heidelberg New York